Effect of Freshwater Inflow on Habitat Suitability Change in Texas Bays

by:

Evan L. Turner, Kelly Savage, Joe Trungale, Terry A. Palmer, and Paul A. Montagna

Harte Research Institute for Gulf of Mexico Studies
Texas A&M University - Corpus Christi
6300 Ocean Drive, Unit 5869
Corpus Christi, Texas 78412
Phone: 361-825-2040
Email: paul.montagna@tamucc.edu

Report to:

Texas Environmental Flows Working Group
and
National Fish and Wildlife Foundation

November 2016

Recommended Citation:

Turner, E.L., K. Savage, J. Trungale, T.A. Palmer and P.A. Montagna. 2016. Effect of freshwater inflow on habitat suitability change in Texas bays. Report to the Texas Environmental Flows Working Group and National Fish and Wildlife Foundation. Harte Research Institute, Texas A&M University-Corpus Christi, Corpus Christi, Texas. 35 pages.

Table of Contents

Abstract

Freshwater inflow is critically important for foundational estuarine invertebrate species such as the Eastern Oyster, *Crassostrea virginica*. This empirical study tests the viability of the proactive management strategy of the release of supplementary freshwater inflow into two Texas bays to increase oyster health. An oyster habitat suitability index was created through regression analyses to test the effect of altered inflows. We demonstrate the inflow requirement to lower salinities from base marine (35 PSU) conditions to polyhaline (25 PSU) conditions is possible within human release activities if directed in Tres Palacios Bay and Caranacahua Bay, Texas. Even small inflow supplements such as 1,500 acre-ft of additional freshwater added during the summer months can enhance oyster health. This health improvement is due to lowering the risk of the oyster parasite *Perkinsus marinus* (Dermo) prevalance by decreasing salinities to between 20 and 25 PSU.

1. Introduction

The Eastern Oyster, *Crassostrea virginica*, is a foundational species that creates habitats in estuaries. Oysters are common in Texas bays. In addition to being a commercial species, the Eastern Oyster is critically important for multiple estuary ecosystem functions (Pollack et al. 2013). The ecosystem functions lead directly to providing ecosystem services that benefit the environment and people. The recent 80-85% world-wide decline in oysters (Beck et al. 2009, zu Ermgassen et al. 2012) has led to great concern that estuaries are also losing vital ecosystem services (zu Ermgassen et al. 2013). Protection and restoration of oyster habitats is a common conservation measure, and a priority focus of the Gulf of Mexico RESTORE program (Deepwater Horizon NRDA Trustees 2016).

While fishing pressure has certainly led to oyster habitat loss, another threat is degradation of water quality, which defines habitat quality for oyster populations. Salinity is often described as a key water quality indicator and predictor of oyster locations and oyster reef health (Bergquist et al. 2006, Turner 2006, Buzan et al. 2006, Pollack et al. 2012). Salinity effects both oysters themselves and predators and diseases because oysters have preferred salinity ranges, and predators and parasites prefer high salinities. Ironically, too much freshwater lowers salinity too far and harms oysters (Turner 2006), and too little freshwater raises salinity too high and harms oysters (Buzan et al. 2006). Thus, there is a salinity zone in the middle that constrains oyster population's growth, survival and distribution within estuaries.

Salinity in estuaries is controlled by a combination and interaction between climate (that drives river flow) on one end, and geomorphology and tidal range (that drives salt water exchange) on the other end (Montagna et al. 2013). Freshwater inflow is important to estuary health in general because it delivers nutrient (that stimulates primary production) and sediments (needed to build habitats), and dilutes salinity from the river to the sea (which drives salinity gradients within estuaries). However, salinity is often altered when freshwater is diverted from estuaries and put to use by humans for municipal, industrial, and agricultural purposes. So, it is necessary to know how much environmental flow is necessary to maintain estuary conditions necessary to maintain health of oyster populations. This information can also be useful for planning conservation programs designed to protect or ensure environmental flow regimes needed to protect, restore, or enhance oyster reefs.

The goal of the current project is to describe a model of oyster health based on salinity and freshwater inflow. The approach is to construct a model of oyster health from long-term observations of the oyster parasite *Perkinsus marinus*, commonly referred to as Dermo. Dermo is used to describe both the *Perkinsus marinus* parasite and the physical tissue destruction caused on the Eastern Oyster. In addition to increasing oyster mortality and lowering reproduction, *Perkinsus marinus* affects the local fisheries economy by greatly reducing the value of harvested oysters with diseased flesh (Andrews 1988). By modeling the prevalence and intensity of Dermo infection among Texas *Crassostrea virginica* habitats a simulation model can be constructed to inform managers of estuary conditions favorable for oyster habitat. Additionally, a habitat suitability index is constructed to provide qualitative metrics on the overall estuary oyster health.

2. Methods

Model development was followed by model calibration. Data for the calibration was obtained from several existing sources and new data collections as described below. Several submodels were developed, which were combined to create a habitat suitability index (HSI). Finally, the HSI was calculated for various inflow scenarios.

2.1. Long-Term Texas Oyster Data and Analyses

Oyster and hydrographical data were obtained for the Mission-Aransas Estuary. A Mission-Aransas National Estuarine Research Reserve (MANERR) long-term hydrographical station in eastern Copano Bay (Copano Bay East, MARCEWQ, 28.1323 °N, 97.0344 °W) was selected for the point of calibration along with the three nearest long-term Dermo collection stations (Fig. 1). Salinity, temperature, pH and dissolved oxygen observations have been measured continuously since 2007 (Fig. 2.). Oyster data, including Dermo prevalence was collected by Dr. Jennifer Pollack, TAMUCC and Dermo data can be downloaded from the Oyster Sentinel database http://www.oystersentinel.org/ (Ray, 2016). The three nearest Dermo monitoring stations to the Copano East hydrological station are Lap Reef (28.13459 °N, -97.0543 °W), NW Causeway Reef (28.12789 °N, 97.0163 °W), and SW Causeway Reef (28.11845 °N, 97.0248 °W). These reefs have also been systematically sampled for oyster size and abundance by Texas Parks and Wildlife Department (TPWD) since 1986 (TPWD, 2015). Hydrographical data were compared with oyster health and later used as a calibration set for the modeling activities.

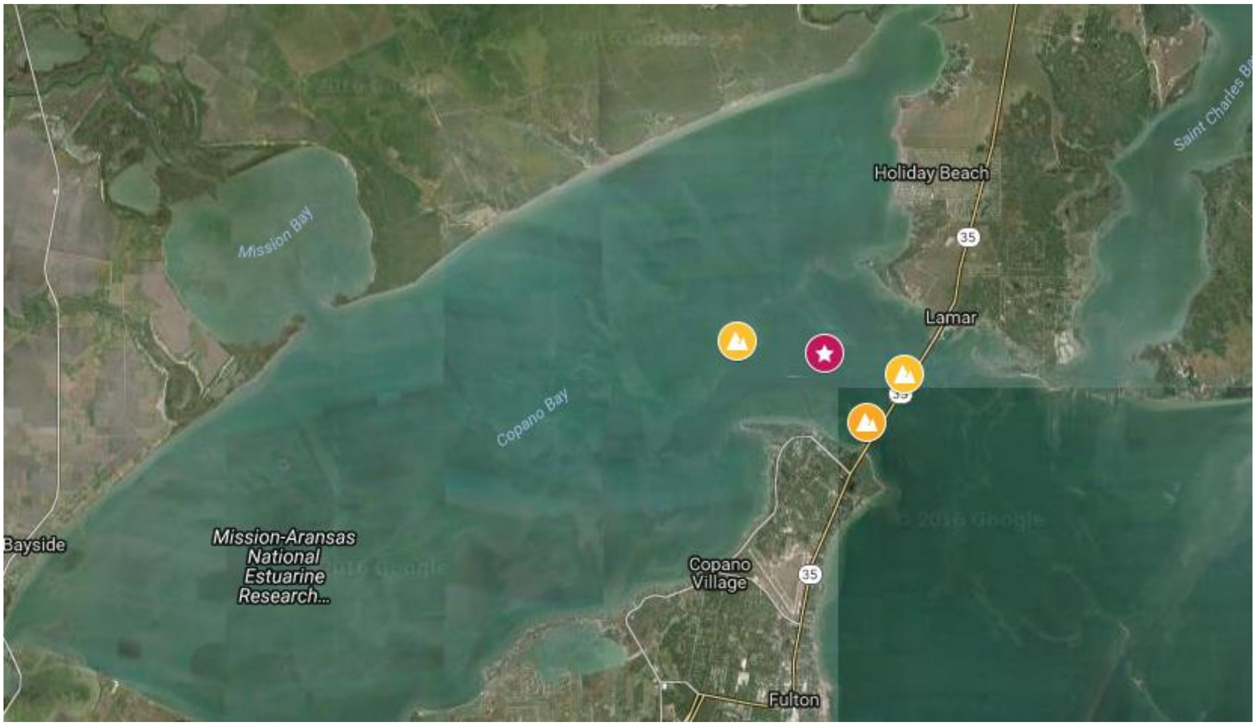

Fig. 1. Location of Dermo Severity Index calibration data stations in the Mission-Aransas Estuary. The hydrographical observation point, depicted by a red star, is the MANERR station Copano Bay East. The three closest long-term Dermo observation oyster beds are depicted with yellow symbols.

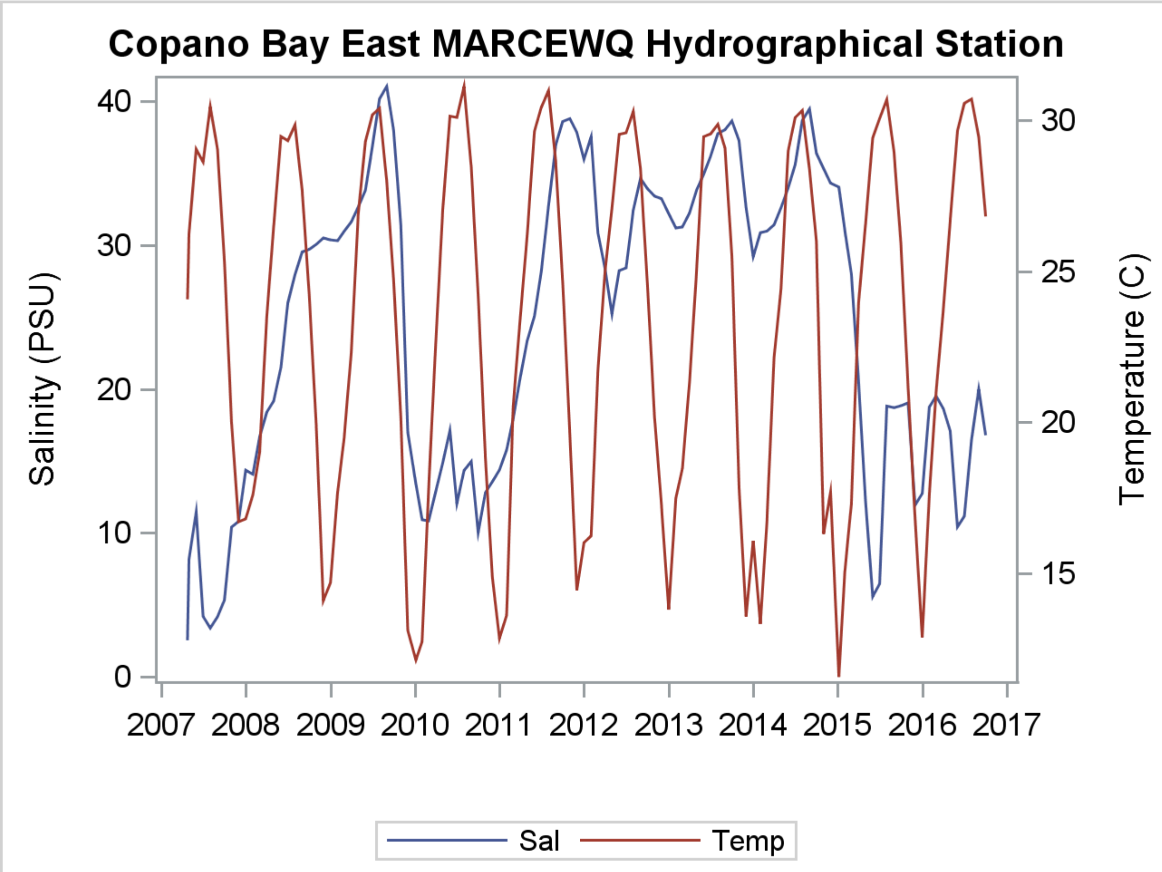

Fig. 2. Copano Bay East MARCEWQ station monthly average salinity and water temperature from April 2007 to April 2016. Abbreviations: Sal = salinity, Temp = Temperature.

2.2. Pekinsus marinus (Dermo) Relationship to Physical Factors

Pekinsus marinus (Dermo) infection was measured by counting the number of oysters with infection and grading the infection intensity. These methods are detailed in (Ray, 1966). A simple infection index is created by multiplying the percentage of infected individuals by the average intensity. This is a common technique that normalizes Dermo observation studies where the number of individuals sampled can be variable. This metric, the weighted prevalence, is given as:

Eq. 1. $$Weighted\ Prevelance = \%Infected * Dermo\ Intensity$$

A combination of linear regressions and upper quantile analysis regressions were employed to discover the relationship to Dermo prevalence to physical factors. First, a simple linear regression was employed to the entire dataset. Second, a quantile linear regression at the 90th percentile (P) is used to explore the effects of the physical variable at the higher quantile levels. Last, a nonlinear log-normal equation is fit to the dataset using the Max Bin approach. The Max Bin method provides similar results to a quantile regression at the P90 to P95 level and allows for the regression of nonlinear equations (Turner and Montagna 2017). The model can be used to characterize the nonlinear relationship between biological characteristics where dependent variables could be abundance, biomass, or diversity and the independent variables could be salinity, temperature, or depth. The three parameters characterize different attributes of the curve, where *a* is the peak of the dependent value (*Y*-axis), *b* is the skewness or rate of change of the response as a function of *X*, and *c* the optimal value of the independent variable on the *X*-axis (Montagna et al. 2002b) (Eq. 2).

Eq. 2 $$Y = a \times \exp\left(-0.5 \times \left(\ln \frac{\left(\frac{X}{c}\right)}{b}\right)^2\right)$$

The same procedures described above were repeated on observations for oyster average oyster length to salinity and water temperature using the expanded TPWD oyster dataset for the reefs from 1978 to 2015.

Weighted Dermo intensity of adult sized > 25 mm oysters was found to be weakly related to salinity and water temperature using a linear regression method at an R^2 value of 0.34 and 0.09, respectively (Fig. 3 and Fig. 4). The lognormal coefficients fit by the Max Bin method for Dermo intensity to salinity are *a* = 2.756, *b* = 1.058, and *c* = 33.367. The respective coefficients for the temperature regression are: *a* = 2.737, *b* = 0.6024, and *c* = 29.729.

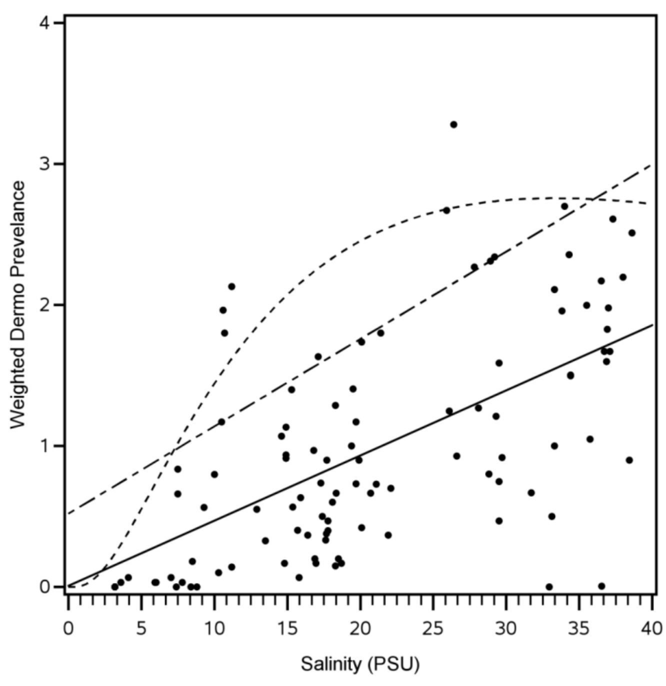

Fig. 3. Regression of weighted Dermo intensity of adult sized (> 25mm) oysters for east Copano Bay from Dec 2007 to Apr 2016 given observed salinity (PSU). The solid line represents the least squares regression at r^2 = 0.34. The dashed line represents the quantile regression at P90. The dotted line represent the optimal salinity using the Max Bin method.

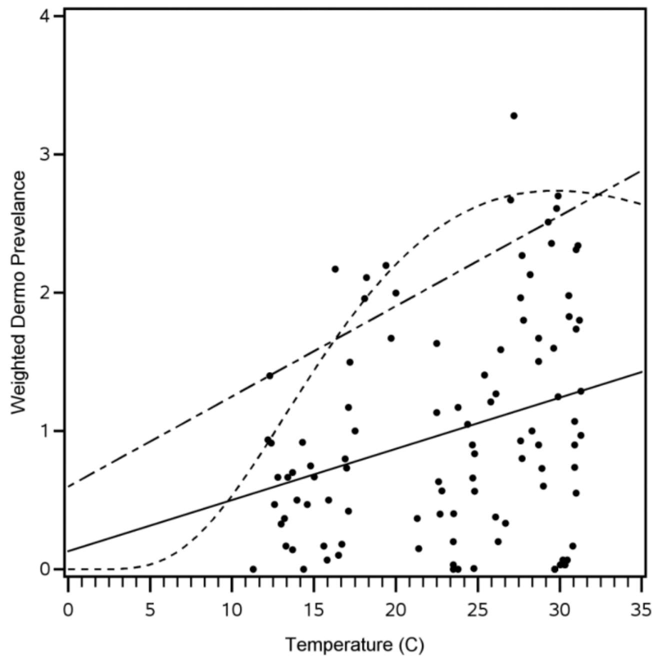

Fig. 4. Regression of weighted Dermo intensity of adult sized (> 25mm) oysters for East Copano Bay from Dec 2007 to Apr 2016 with observed water temperature. The solid line represents the least squares regression at $r^2 = 0.09$. The dashed line represents the quantile regression at P90. The dotted line represent the optimal salinity using the Max Bin method.

2.3. Oyster Length-Salinity Relationship

The average length of adult (> 25mm) oysters were not significantly related with either salinity or water temperature using a linear regression method ($R^2 = 0.07$ and .002, respectively; Fig. 5 and Fig. 6). The log-normal coefficients fit by the Max Bin method for average length to salinity are $a = 111.577$, $b = 1.522$, and $c = 10.02$. The respective coefficients for the temperature regression are: $a = 108.355$, $b = 1.81507$, and $c = 34.96$.

Oyster juveniles (spat) numbers were also regressed with salinity. The linear relationship had an R^2 value of 0.03 with the Max Bin lognormal coefficients $a = 109.613$, $b = 0.30511$, and $c = 21.65$ (Fig. 7).

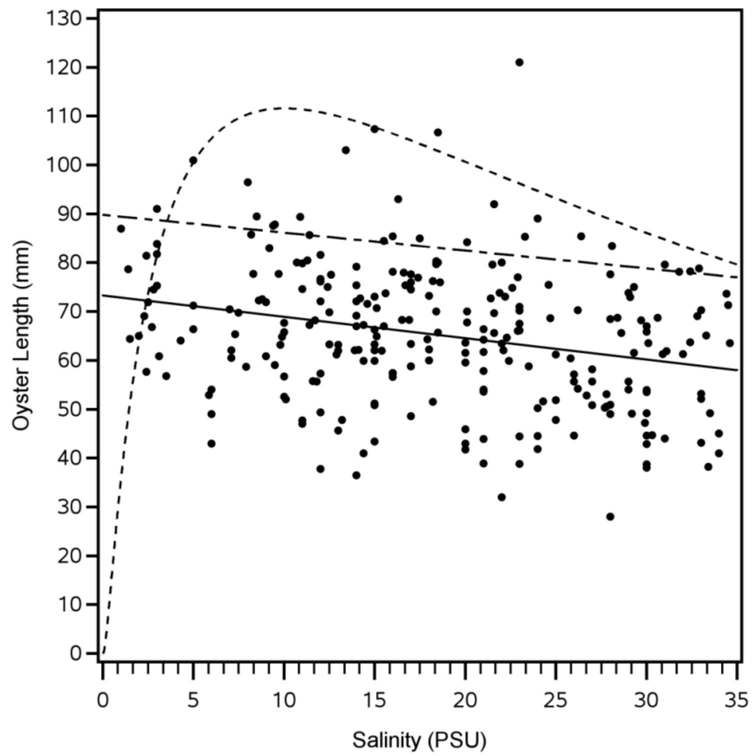

Fig. 5. Oyster length regression with salinity for East Copano Bay from 1979 to 2015.

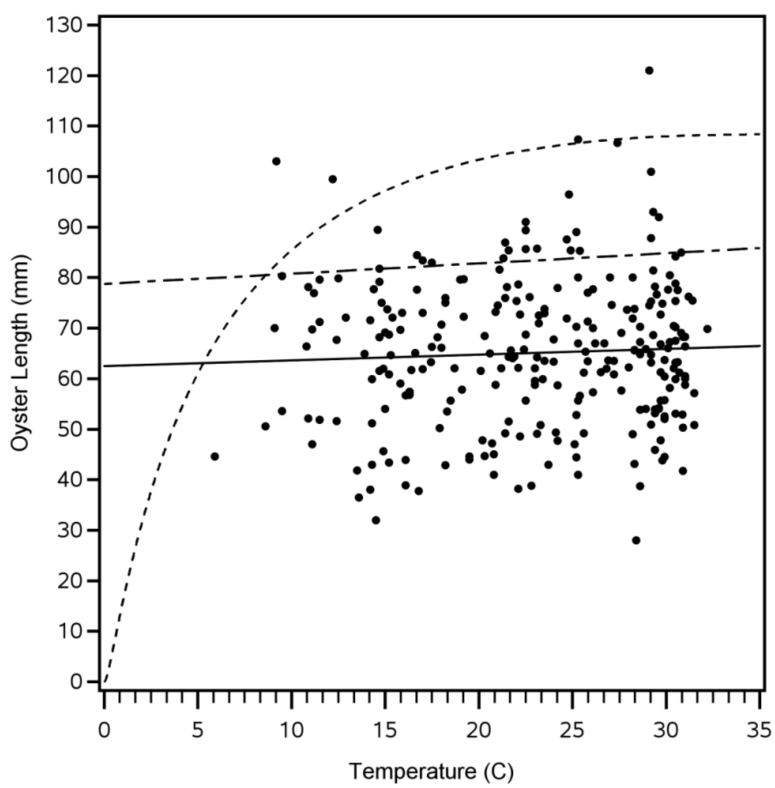

Fig. 6. Oyster length regression with temperature for East Copano Bay from 1979 to 2015.

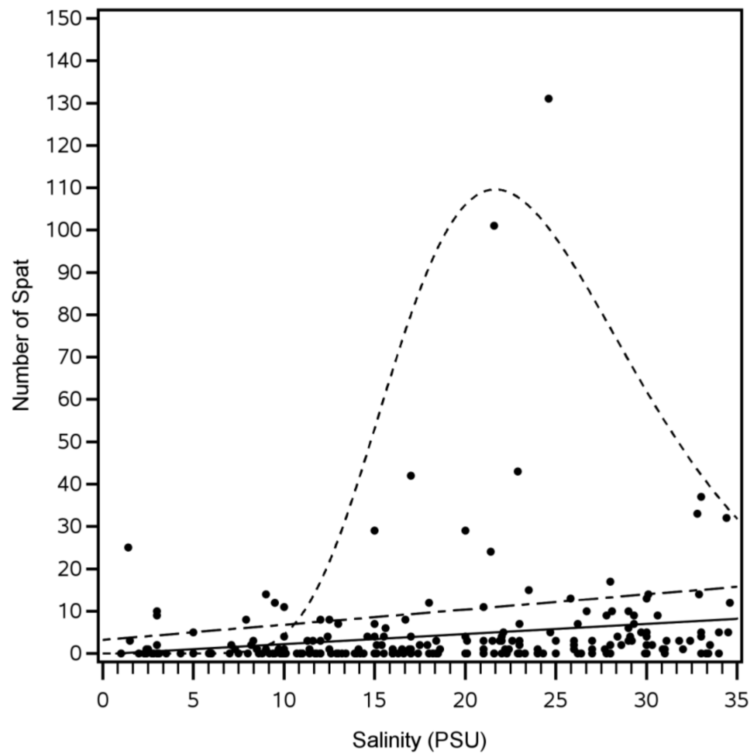

Fig. 7. Oyster spat (juveniles) abundance regression with salinity for East Copano Bay from 1979 to 2015.

2.4. Texas Dermo Risk Model (TDRM)

The Texas Dermo Severity Risk Model (TDRM) was developed using a regression-based approach from *Perkinsus marinus* observations in the Texas coast. The TDRM is a metric that can be applied to hydrographical observations of Texas estuaries for the purposes of evaluating oyster habitat suitability and risk mitigation.

The model was constructed by adapting the nonlinear log-normal Eq. 2 analysis performed on Dermo intensity to salinity and water temperature. The premise of the model design is each both salinity and water temperature are driving factors of Dermo intensity. In regression analysis, salinity was found to be the strongest driver of Dermo intensity, while water temperature acts as a catalyst. For example, water temperature has no effect on Dermo at low salinities, but during periods of high salinity may exacerbate the Dermo intensity. The full model equations and variables are listed in Table 1.

Table 1. Equations for the Texas Dermo Risk model. A. Equations. B. Variable definitions.

A.

Equations	Description
$TDRM = SR * TR$	Dermo Risk Model
SR= $Sa \times \exp\left(-se \times \left(\ln\frac{\left(\frac{Salinity}{sc}\right)}{sb}\right)^2\right)$	Salinity Risk
TR= $Ta \times \exp\left(-te \times \left(\ln\frac{\left(\frac{Temperature}{tc}\right)}{tb}\right)^2\right)$	Temperature Risk

B.

Variable	Definition	Units
TDRM	Dermo Intensity	Dermo Intensity (0 – 5)
SR	Salinity Dermo Intensity	Dermo Intensity (0 – 5)
TR	Dermo Temperature Scaling	Unit less
salinity	Salinity	PSU
temperature	water temperature	°C
sa	Salinity Amplitude	Dermo Intensity
sb	Salinity Skewness	Unit less
sc	Salinity Maximum	PSU
se	Salinity Exponential	Unit less
ta	Temperature Amplitude	Dermo Intensity
tb	Temperature skewness	Unit less
tc	Temperature Maximum	C
te	Temperature Exponential	Unit less

2.4.1 TDRM Calibration

The Texas Dermo Risk Model is calibrated using daily averages of hydrographical observations at Copano Bay East (Fig. 1). The Dermo intensity collections for the three nearest oyster reef stations were used as a validation set for the goodness of fit. Among the constants used for the TDRM, many of the values are already defined either by the natural environment of the study site or discovered during the regression analysis. For example, the maximum salinity and water temperature for the area was defined at 45 PSU and 35 °C respectively. Additionally, since the Dermo intensity metric is a qualitative scale that ranges from 0 to 5, the amplitude of salinity, s_a, is set to equal 5.0. The amplitude of temperature, t_a, is consequentially allowed to vary from 0 to 1 in order to normalize the temperature affect. Finally, the skewness of the log-normal equations (coefficient *b* in Eq. 2.) is set equal to the values of the regressions explored in the analysis of the respective physical conditions to Dermo intensity. Values for t_e and s_e were calculated using a non-exhaustive brute force calibration to the observational dataset to minimize the Root Mean Square Error (RMSE) and % Mean Absolute Error (MAE) of the residuals (Eq. 3 and Eq. 4).

Eq. 3.
$$RMSE = \sqrt{\frac{\sum_{i=1}^{n}(X_{obs,i} - X_{model,i})^2}{n}}$$

Eq. 4.
$$\%MAE = \frac{\sum_{i=1}^{n}\left|X_{obs,i} - X_{model,i}\right|}{\sum_{i=1}^{n} X_{model,i}} * 100$$

The model was fit to the observation points using a brute force non-exhaustive calibration search of the calibration points. Approximately 30,000 runs of the algorithm achieved a MAE of 48.6% and RMSD of 0.675. Therefore, the model fit to 51.4% of the deviation of the observations (Fig. 8). Full calibration constants of the TDRM are listed in Table 2.

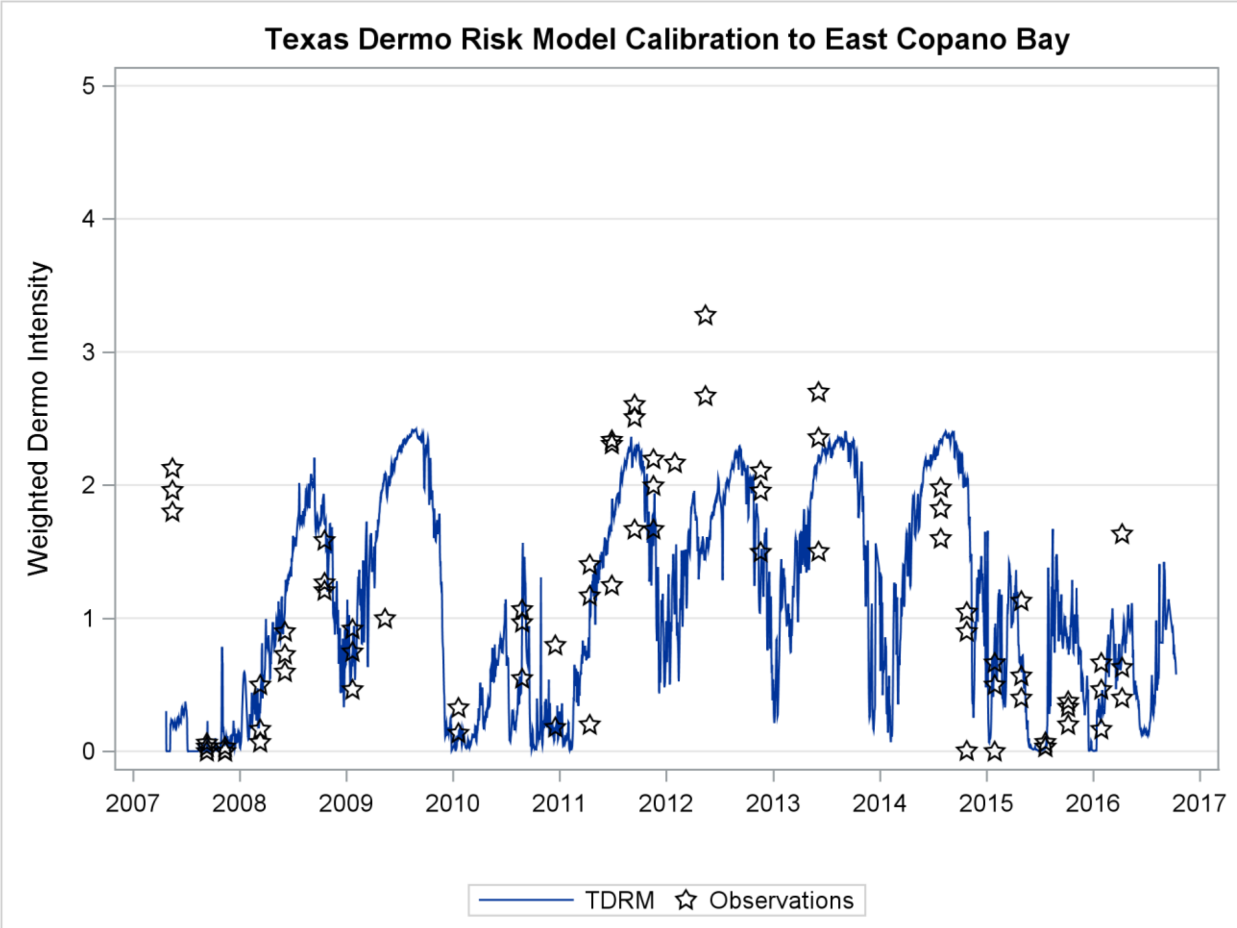

Fig. 8. Dermo Severity Model of the East Copano Bay hydrographical station for 2007 through 2016 plotted alongside the weighted Dermo infection intensity of adult (> 25 mm) oysters. The TDRM model fit the observations with a MAE of 48.6% and RMSD of 0.675.

Table 2. Texas Dermo risk model calibration constants.

Variable	Value	Units
sa	5	Dermo Intensity (0 – 5)
sb	1.05856	Unit less
s_c	45	PSU
se	-1.3	Unit less
ta	0.5	Dermo Intensity (0 – 5)
tb	0.6024	Unit less
tc	35	°C
te	-0.5	Unit less

2.4.2 TDRM Model Validation and Application

In July 2016 Eastern Oyster Dermo samples were collected at multiple previously known and unknown reef locations in the Carancahua and Tres Palacios Bays. These reef stations extend to near the previously defined water quality stations N1, N2, and N3 that were monitored from September 2015 to September 2016. In total, 10 reefs were sampled for Dermo prevalence using the previously described methods (Ray, 1966) (Fig. 9).

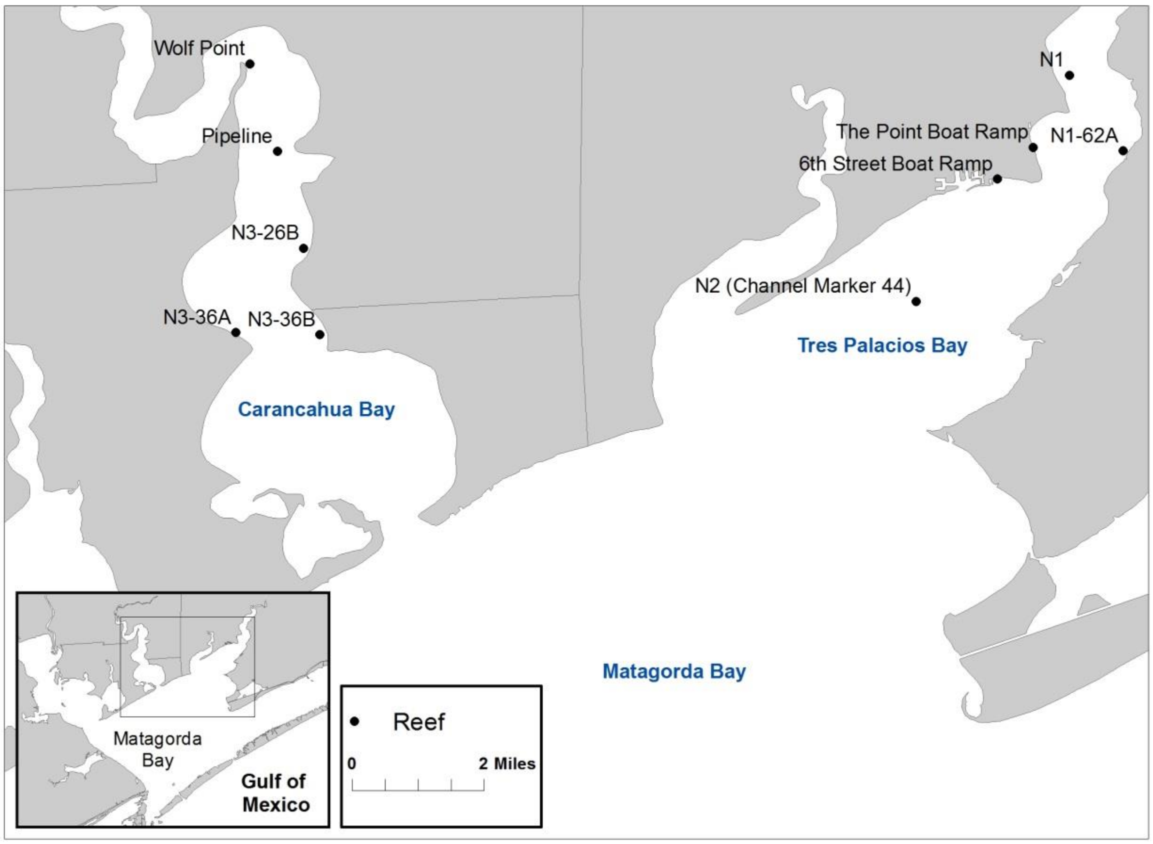

Fig. 9. Oyster reef stations sampled for Dermo prevalence in July 2016.

The Dermo intensity measured during collection activities was low (< 0.5) for both juvenile and commercial size oysters. Commercial intensity averaged 0.036 among all sites with maximum 0.2 at station N3-26B. Validating the TDRM using the salinity and water temperature measurements collected on site yielded an estimated commercial Dermo intensity of 0.01 to 0.3 with an average Dermo intensity of 0.16. The difference between actual vs. modeled Dermo intensity was 0.12. Therefore, the TDRM model overestimated the actual Dermo intensity during the sample study on average of 0.12.

By applying TDRM to the hydrographical conditions monitored in Carancahua and Tres Palacios Bays, a hindcast is constructed of Dermo risk. The estimated Dermo intensity in commercial oysters of Carancahua Bay was under 0.5 for the entire period (Station N3), while estimated intensity increased during fall 2015, spring 2016, and late summer 2016 in Tres Palacios Bay (Fig. 11).

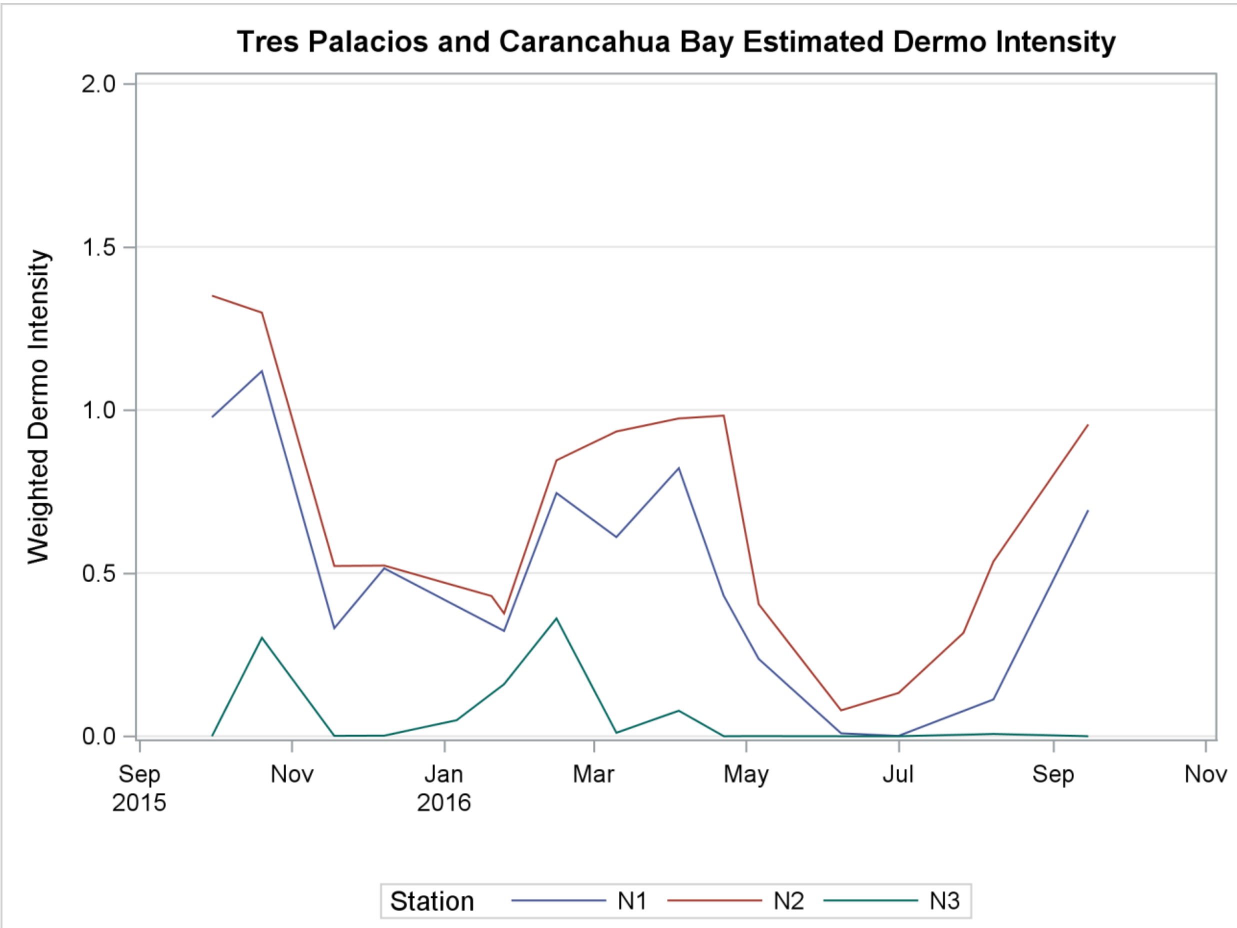

Fig. 11. Texas Dermo Risk Model applied to Carancahua Bay (station N3) and Tres Palacios Bay (Stations N1 and N2) monthly hydrographical observations. The TDRM model was validated to Dermo intensity during July 2016 with an average overestimation error of 0.12.

2.5. Oyster Habitat Suitability Index

In designing an oyster suitability model, existing Habitat Suitability Indexes (HSI) were examined for their utility towards defining optimal flow regimes for South Texas Estuaries. Notably, many existing indices take into factor substrate conditions of suitable clutch for the creation of new reefs, which is not required for projects monitoring existing reefs. The Oyster Sentinel group, for example, maintains an HSI index online for the Gulf of Mexico region (Ray 2016). The elements that were determined to be beneficial to the current index are: salinity during spawning time, minimizing extended periods of low salinity, mean overall salinity, and lowering Dermo risk.

2.5.1 Mean Salinity During Spawning Season

Oyster juveniles (spat) are historically predominant during the spawning months between May and September (Pollack et al. 2011). During the period higher salinities (from 18 to 24 PSU) are optimal (Turner 2006, Pollack et al. 2009). The higher salinity optimal was also observed during the regression analysis of spat to salinity (Fig. 7). Using the log-normal regression coefficients found during analysis a sub-index equation can be constructed to normalize the range of salinity desired during the spawning months. The coefficients to satisfy Eq. 1 are $a = 1$, $b = 0.30511$, and $c = 21.65$. The resulting index equation is visualized as Fig. 12.

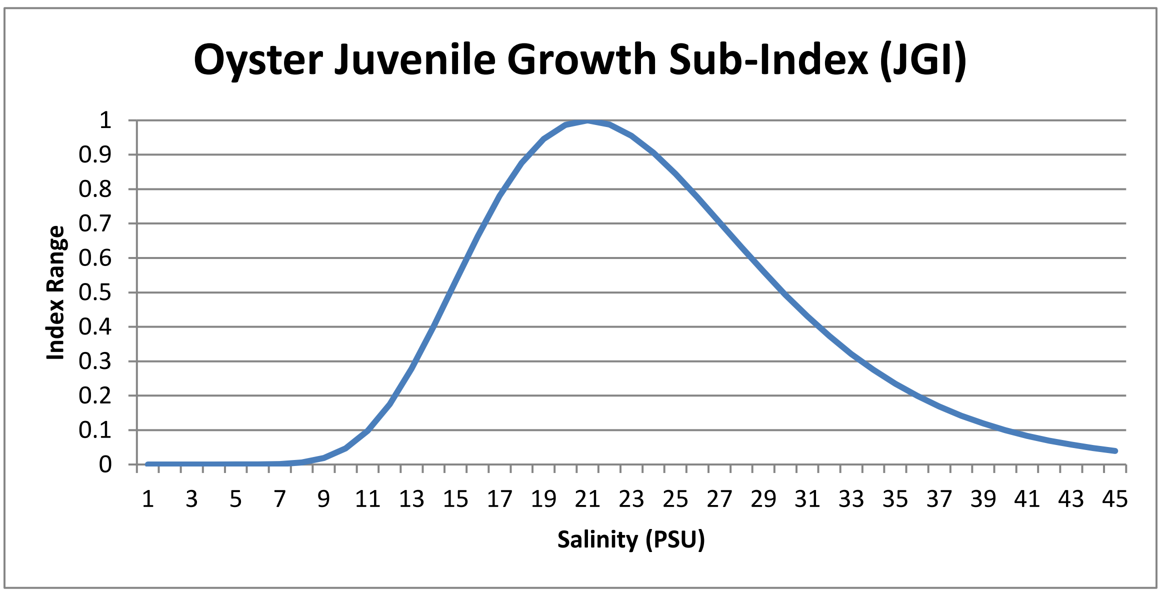

Fig. 12. The Oyster Juvenile Sub-Index. The index approaches 1 when salinities are near 21 PSU during the spawning months (May to September).

To further investigate the average spawning months the TPWD oyster collection database for the entire Texas coast was analyzed between the years 1978 to 2015. The observations for a number of spat collected were first averaged to the date-station level. The residual observations were then averaged by month. According to the this analysis spat were historically the highest on average during the month of July, followed by August, September, and June.

2.5.2 Oyster Salinity Effects Sub-Indices

Extended periods of low salinity (< 2 PSU) are extremely detrimental to oyster health as the Eastern Oyster is not a freshwater species. The general predominant knowledge to date is low salinity (< 2 PSU) on average for a month is fatal to oysters (Barnes et al., 2007; Ray, 2016). However, this effect is negated once salinities rise above 8 PSU on average per month. However, regressions have also shown that oysters can be tolerant to single months of higher salinities (> 30 PSU), but overall annual means should be around 15 PSU to maximize growth.

To simulate these competing effects two Sub-Indexes were created. A Salinity mortality Sub-index is modeled using the lognormal equation regressed for salinity to Oyster length (see Fig. 5). The coefficients utilized are a=1, b = 1.5, and c = 10. A visualization of the salinity mortality sub-index is presented as Fig. 13.

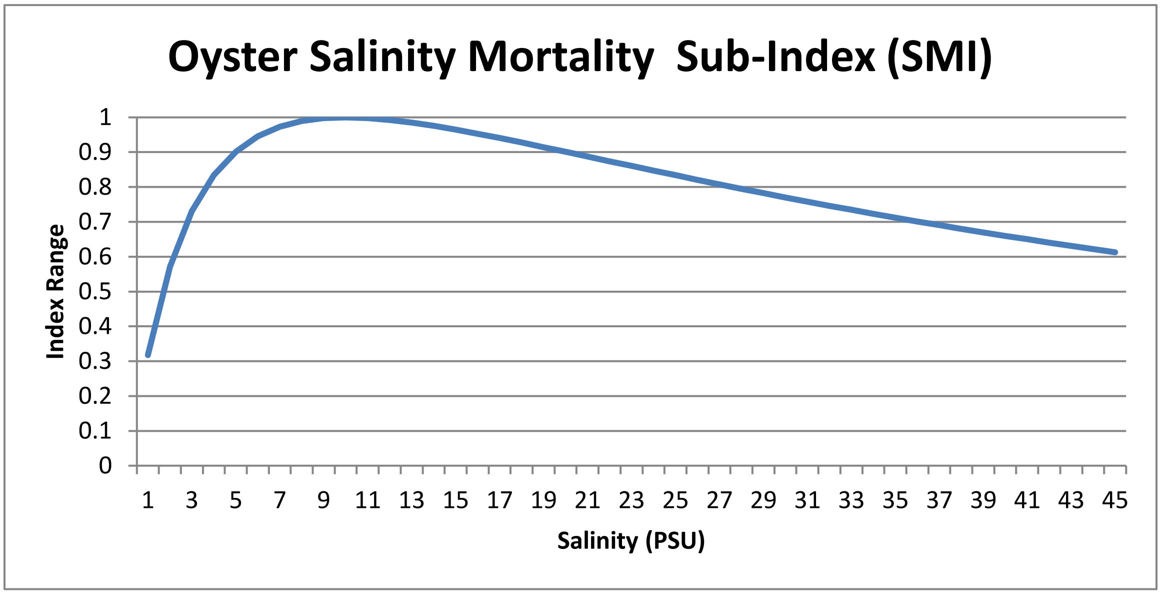

Fig. 13. The Oyster Salinity Mortality Sub-Index. Extremely low < 2 PSU periods are extremely detrimental to oysters while higher salinities have less effect.

Finally, a simple growth sub-index was created using the mean annual average salinity of 12. This index follows closely to other published oyster HSI's (Barnes et al., 2007; Cake, 1983; Soniat et al., 1988; Ray, 2016). The coefficients utilized are a=1, b = 0.5, and c = 12. A visualization of the salinity growth sub-index is presented as Fig. 14.

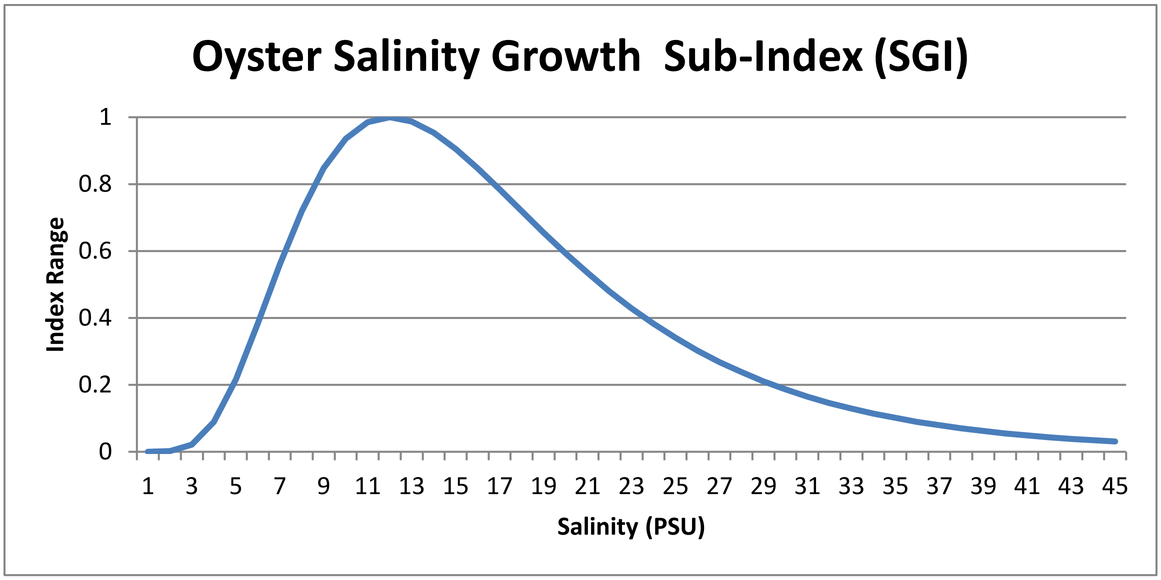

Fig. 14. The Oyster Salinity Growth Sub-Index. The average mean salinity of suitable habitat for the Eastern Oyster is 12 PSU.

2.5.3 Dermo Risk Sub-Index

The output from the Texas Dermo Risk Model is converted to a qualitative risk function to normalize the risk between values of 0 to 1. Additionally, Dermo intensity values < 1 are considered very healthy, while values above 3 are considered severely impacted (Fig. 15). The index is constructed from a Gaussian based exponential:

Eq. 5. $$Dermo\ Severity\ Sub-Index = e^{-0.5*\left(\frac{Intensity}{2}\right)^{2.5}}$$

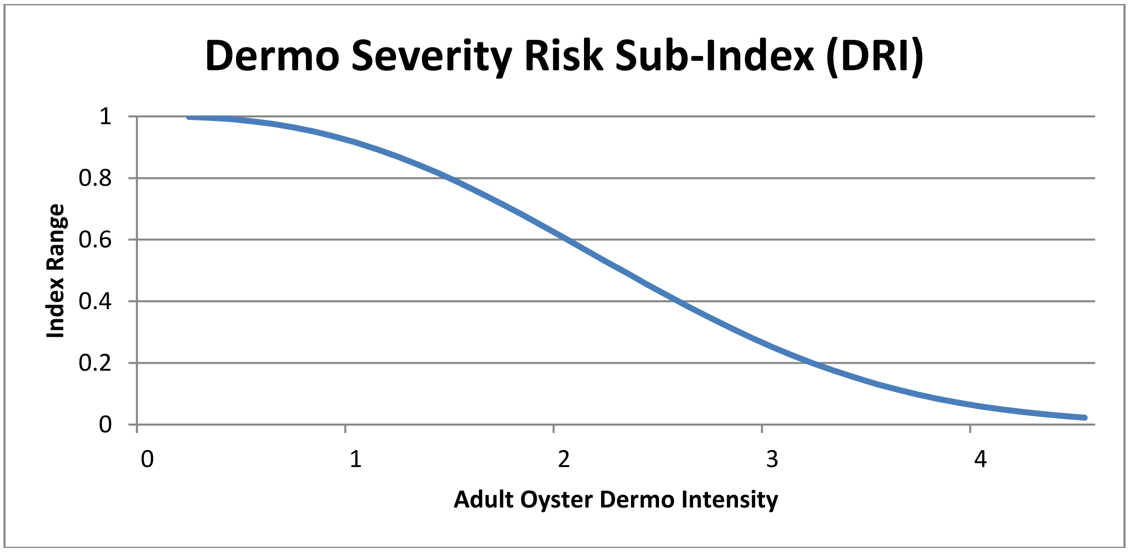

Fig. 15. The Dermo Severity Risk Sub-Index. Adult (> 25mm) oyster Dermo intensities > 3 severely compromise the overall health index of oyster habitats.

2.5.4 Combined Oyster Habitat Suitability Index

The full oyster Habitat Suitability Index (HSI) is a yearly qualitative range from 0 to 10, where 0 being the most inhospitable physical conditions for oyster health to 10 being the most optimal. The score is designed as a yearly index value as specific seasonal trends are addressed, such as the spawning season where oyster juveniles (spat) require salinities above the recommended yearly average. The inputs to the HSI model are monthly mean salinities at reef location and the mean monthly Dermo intensity from the TDRM model. The TDRM model input requires salinity and water temperature to determine Dermo intensity.

For a single yearly index value the lowest monthly sub-indices for salinity mortality (SMI) and juvenile salinity (JGI) are multiplied by the yearly average Dermo severity risk (DRI) and salinity growth (SGI) (see Eq. 6). The juvenile salinity growth (JGI) sub-index is only applied during June, July, August, and September. The full SAS 9.4 code for the HSI is included in Appendix A1.

Eq. 6. $$HSI = (\lfloor SM \rfloor + DR + \lfloor JG \rfloor + SG) * 2.5$$

2.5.5 East Copano Bay HSI Response

The HSI was executed using the existing salinity and Dermo model response numbers for the East Copano Bay station (Fig. 1). The maximum HSI was 8.41 for 2010, with the lowest HSI of 4.34 in 2009 (Fig. 16). Individual scores for each sub-index are listed in Table 2 and visually represented in Fig 17.

Table 3. Habitat Suitability Index of East Copano Bay.

Year	**Avg. Salinity**	**HSI**	**Sub-Indices**			
			DRI	**SGI**	**JGI**	**SMI**
2007	6.71	5.49	1.00	0.51	0.03	0.66
2008	23.16	7.21	0.92	0.42	0.78	0.76
2009	32.66	4.34	0.76	0.13	0.20	0.64
2010	13.19	8.41	1.00	0.98	0.45	0.94
2011	27.53	5.83	0.87	0.25	0.55	0.66
2012	31.85	5.29	0.77	0.15	0.52	0.68
2013	34.16	4.39	0.75	0.11	0.23	0.67
2014	33.97	4.43	0.77	0.11	0.23	0.66
2015	18.53	7.17	0.99	0.69	0.45	0.75
2016	16.15	7.93	0.99	0.84	0.45	0.90

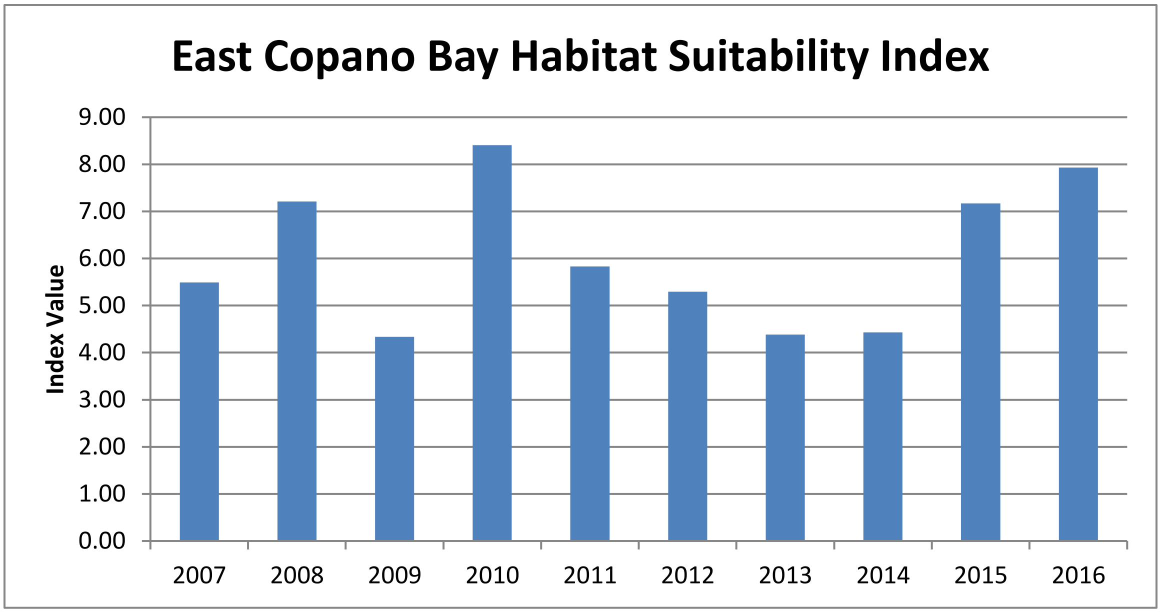

Fig. 16. Oyster Habitat Suitability Index scores per year for East Copano Bay, Texas.

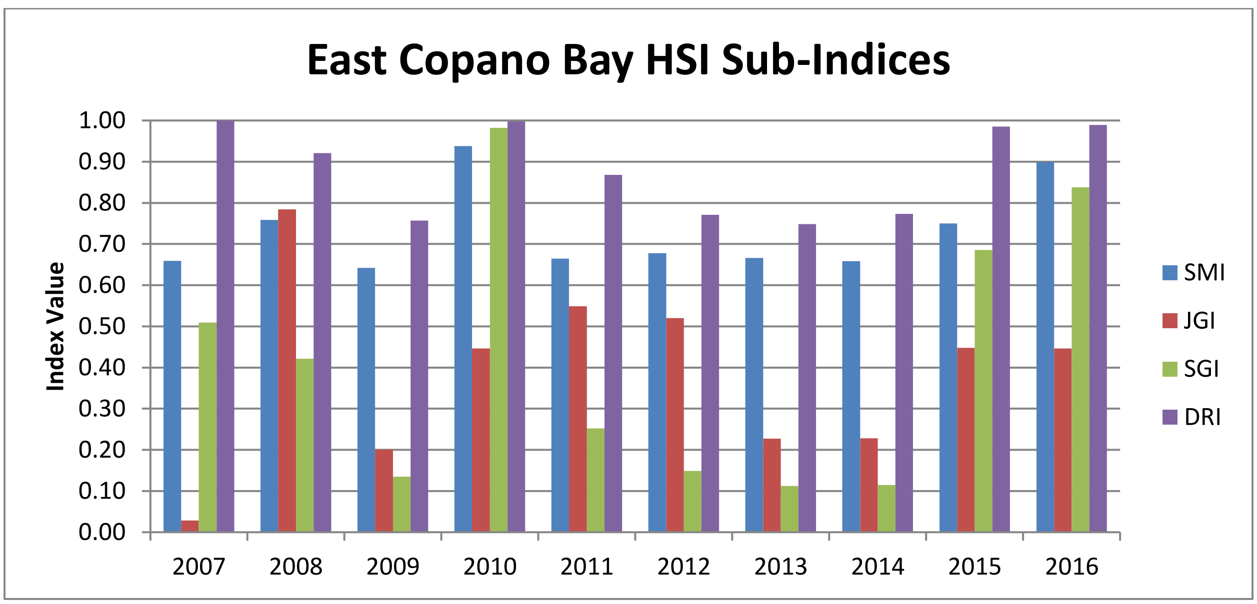

Fig. 17. Individual sub-index scores for the oyster habitat suitability index for East Copano Bay,.

2.6. Inflow Scenario Testing for Tres Palacios and Carancahua Bays, Texas

The ability to define inflow scenarios to oyster health models is of critical importance to determine the amount of freshwater inflow required to an estuary system to maintain proper health. In this activity regressions of inflow (acre-ft/mo) are used to calculate salinity (PSU) near reef sampling stations in the Carancahua Bay and Tres Palacios Bay, Texas (see Fig 9). The method employed is by estimations using the TWDB TXBLEND model (Matsumoto, 1993). The TXBLEND model nodes CAR17, PAL9, and PAL13 correspond to previously sampled stations N3, N1, and N2. TXBLEND node CAR17 is equidistant from stations N3_36A and N3_36B (see Fig. 9) and will be referred to as station N3AB.

Regressions were performed on estimated inflow to model response salinity from TXBELND model runs from 1987 to 2015 (Table 3.). The regression equation outputs salinity (PSU) as a function of inflow (ac-ft/mo) and is represented as:

Eq. 7. $$\mathrm{Salinity} = \mathrm{a} + \mathrm{b} * \log(\mathrm{inflow}) + \mathrm{c} * \log\,(\mathrm{inflow})$$

Conversely, solving for inflow (ac-ft/mo) as a function of salinity (PSU) using the same coefficients yields:

Eq. 8. $$Inflow = \left(e^{Salinity-a}\right)^{\frac{1}{b+c}}$$

Table 3. Coefficients for inflow-salinity regression equations for Tres Palacios and Carancahua Bay, Texas monitoring stations.

Bay	**Station**	**TXBLEND Node**	**R^2**	**Coefficient**	**Value**
Tres Palacios	N1	PAL9	0.62	a	41.7183
				b	-1.5963
				c	-1.1781
	N2	PAL13	0.52	a	46.7045
				b	-1.0929
				c	-1.6494
Carancahua	N3	CAR13	0.80	a	46.7301
				b	-2.0270
				c	-1.7615
	N3AB	CAR17	0.75	a	53.3390
				b	-1.9810
				c	-2.0325

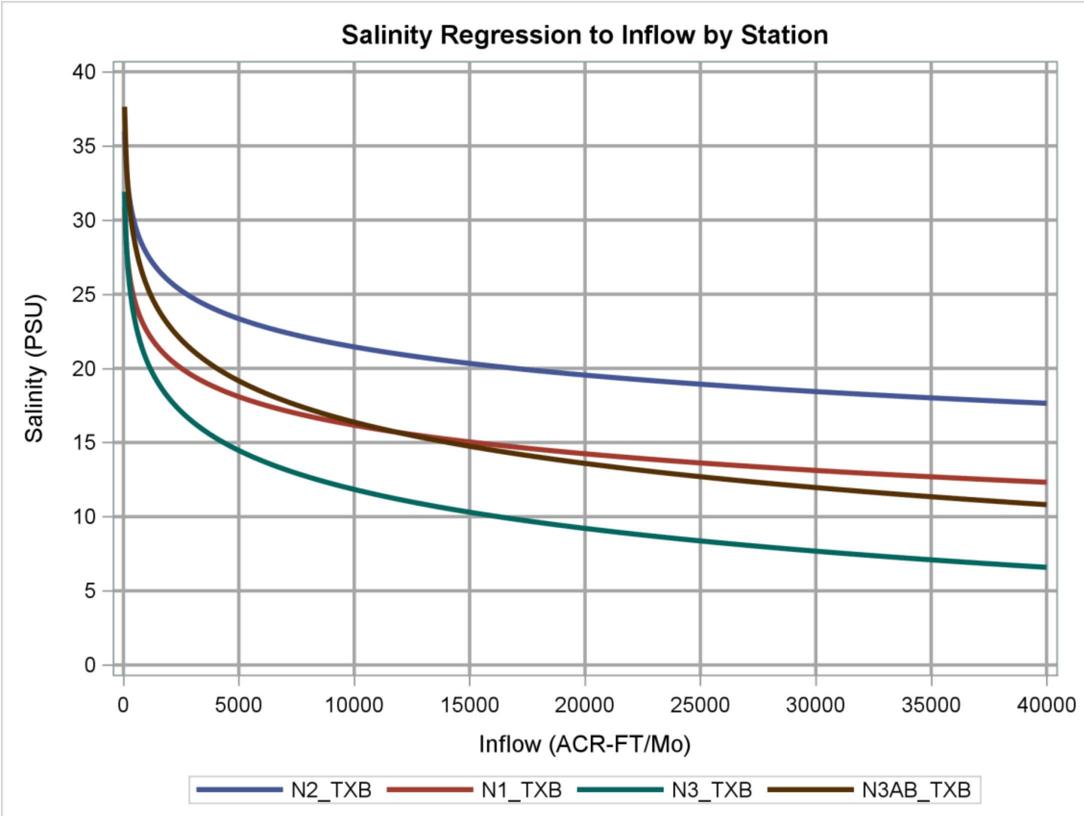

Fig. 18. Inflow salinity regression equations derived from TXBLEND model output from 1986 to 2015 in Tres Palacios Bay and Carancahua Bay, Texas.

A series of simulations are evaluated using the TXBLEND model historical average inflow outputs. The baseline output, or the historical averages, is the completed HSI scores in Fig. 19 A, B, C, and D and A.2. For each scenario, an additional 500, 1,000, and 5,000 ac-ft of inflow is added monthly to the historical record for a seasonal quarter per year. In total, there are 12 scenarios.

The seasonal quarters are:

- Summer: June, July, and August
- Fall: September, October, November
- Winter: December, January, and February
- Spring: March, April, and May

3. Results

3.1. Tres Palacios Bay and Carancahua Bay, Texas Habitat Suitability Index

Evaluating the Tres Palacios and Carancahua Bay stations TXBLEND estimated monthly salinity at sample stations N1, N2, N3, and N3AB found the lowest average monthly sub-index values between June to September (Fig. 19A, B, C, and D). The lowest HSI score year was 2007 when very low contiguous salinities during spawning months lowered the scores for the JGI and SMI sub-indices. The full yearly HSI scores and sub-index scores are included as A.2. The overall average yearly HSI score for each sample location from 1987 to 2015 is 7.85, 6.91, 7.53, and 7.67 respectively for stations N1, N2, N3, and N3AB. Station N2 has the lowest overall HSI score due to lower higher on average salinities throughout the year (SGI) (See Fig. 19B). Station N3 has the highest overall HSI scores on average, but low scores for Juvenile recruitment (JGI) and increased risk of oyster die-off due to sustained low salinities (SMI).

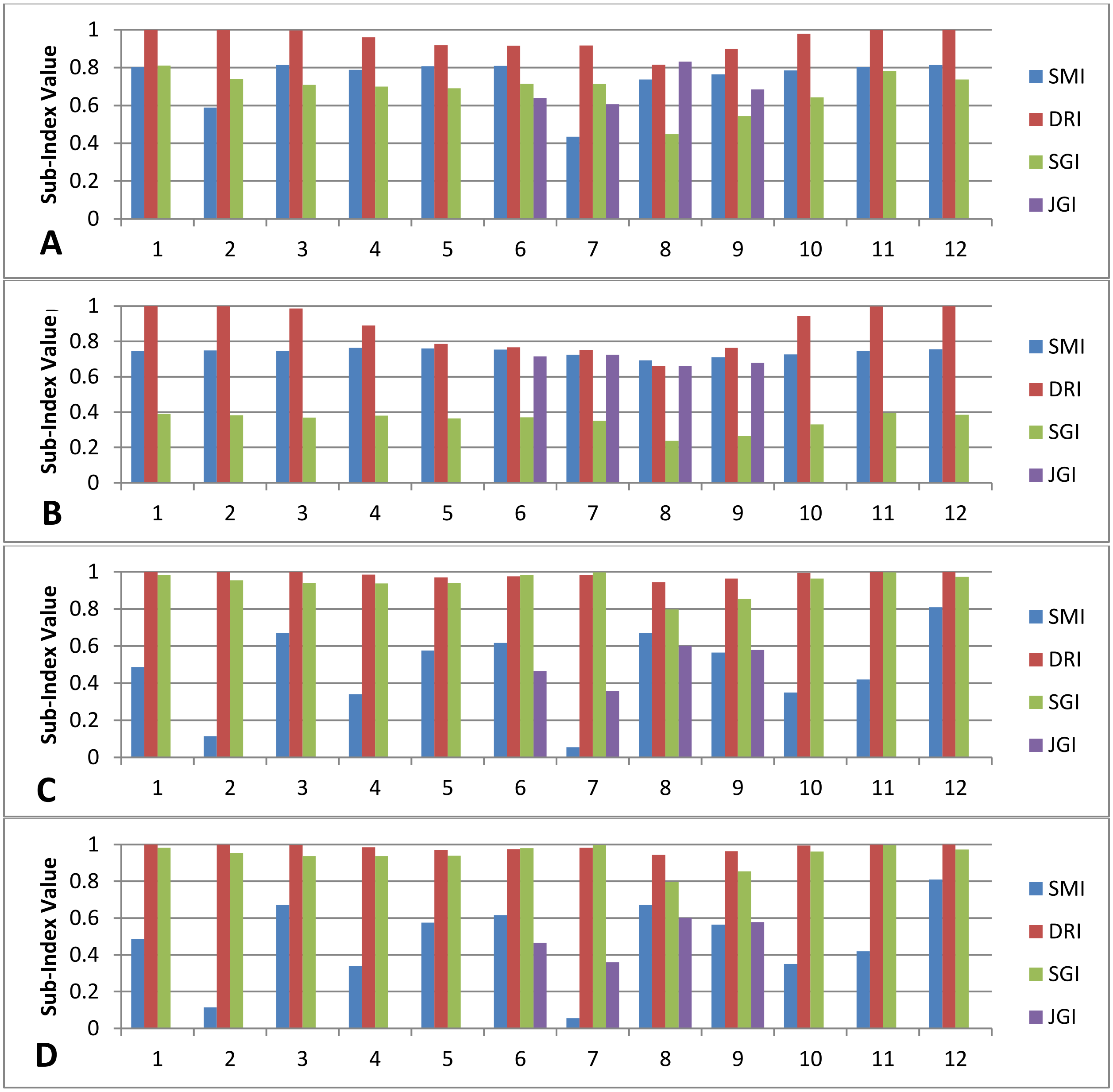

Fig 19. Habitat suitability average monthly sub-index values for Tres Palacios and Carnacahua Bays, Texas from 1986 to 2015 for A) station N1, B) station N2, C) station N3, and D) station N3. Abbreviations: SMI = sustained low salinities subindex, DRI = Dermo risk subindex, SGI = salinity growth subindex, and JGI = juvenile recruitment subindex.

The inflow (ac-ft/mo) regression to salinity (PSU) was transformed into a regression of inflow (ac-ft/mo) to HSI sub-indices by solving each sub-index equation per inflow per station. The salinity mortality sub-index is not solved due to the very high inflows required to sustain a monthly average salinity under 2 PSU requiring the function to be out of range (> 100,000 ac-ft/mo). By solving each inflow to HSI equation a theoretical optimal inflow per month is found for each bay-station to maximize the HSI index value. The salinity growth sub-index is annually based, but solving for monthly average (SGI) optimal values for N1 > 40,000 ac-ft/mo, N2 > 40,000 ac-ft/mo, N3 = 9,600 ac-ft/mo, and N3AB = 29,750 ac-ft/mo (Fig. 20). The Dermo risk subindex (DRI) functions increase indefinitely approaching 1 as inflow increases. However, Dermo risk decreases significantly for all stations where inflow > 5,000 ac-ft/mo (Fig. 21). The juvenile growth sub-index is computed for months June, July, August, and September. The optimal monthly average inflow values for each station reach an optimal state of N1 = 1,400 ac-ft/mo, N2 = 9,300 ac-ft/mo, N3 = 750 ac-ft/mo, and N3AB = 2,700 ac-ft/mo (Fig. 21).

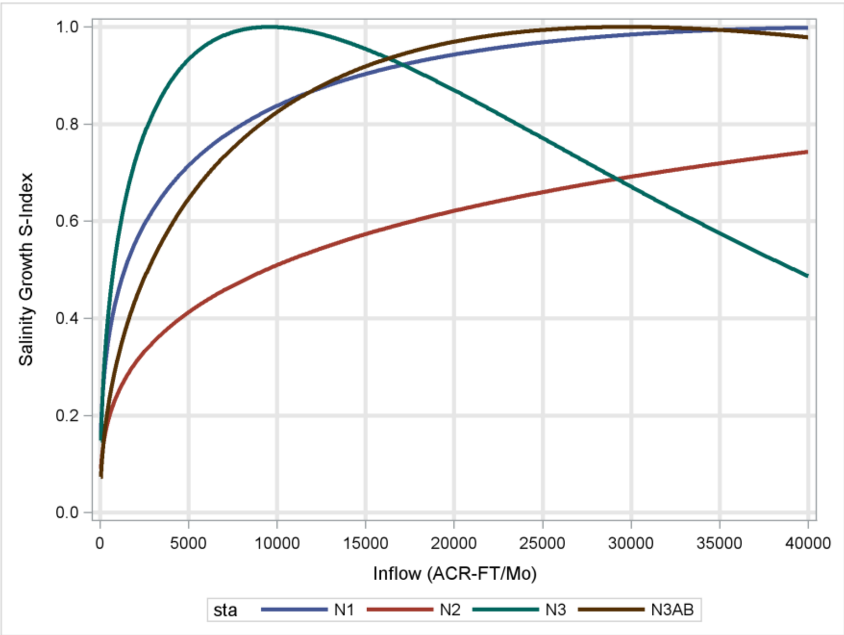

Fig. 20. Regression of salinity growth sub-index (SGI) to inflow (acrft/mo). Optimal values for inflow are N1 > 40,000 ac-ft/mo, N2 > 40,000 ac-ft/mo, N3 = 9,600 ac-ft/mo, and N3AB = 29,750 ac-ft/mo.

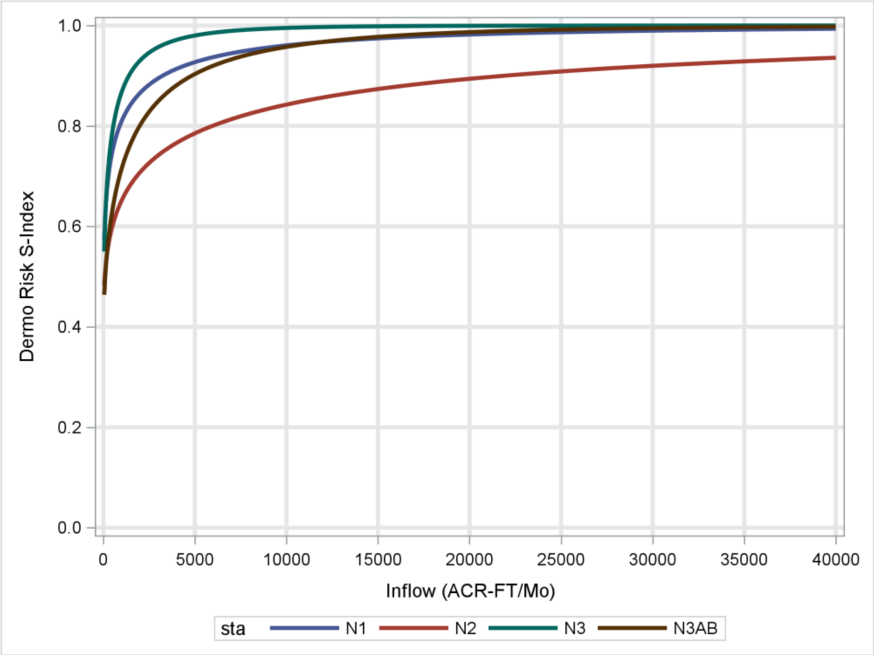

Fig. 20. Regression of Dermo risk sub-index (DRI) to inflow

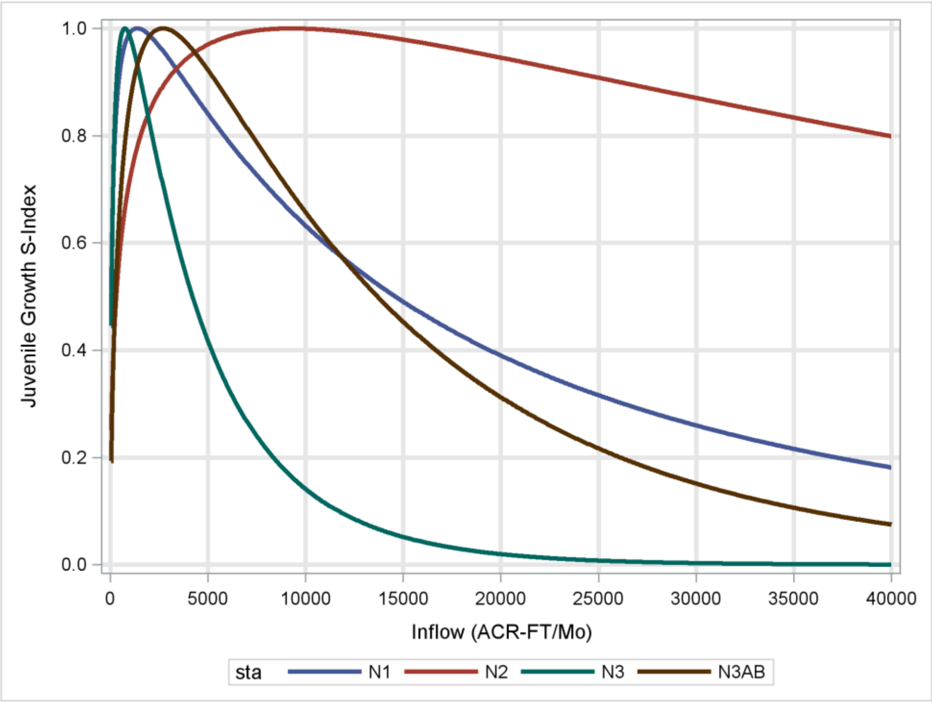

Fig. 21. Regression of oyster juvenile growth index (JGI) to inflow (ac-ft/mo). Optimal inflow for each station is N1 = 1,400 ac-ft/mo, N2 = 9,300 ac-ft/mo, N3 = 750 ac-ft/mo, and N3AB = 2,700 ac-ft/mo.

3.2. Inflow Scenario Testing Results

Each station inflow regression was tested for habitat suitability index based on supplementing existing historical flows with 500, 1000, and 5000 ac-ft/month for a three-month period depending on the quarter. Each run is an average yearly response of each historical year from 1987 to 2015. The most significant HSI gains were made in stations N1 and N2 supplementing 500 ac-ft of freshwater inflow for June, July, and August (Table 4.).

Table 4. Oyster Habitat Suitability Index (HSI) scenarios based on adding 500, 1000, and 5000 acreft of inflow per month for a three-month period. Period zero is the baseline historical TXBLEND model results.

Season	**Station**	**Additonal Monthly Flow (ac-ft)**			
		0	**500**	**1000**	**5000**
Summer	N1	7.73	8.04	8.07	7.91
	N2	7.07	7.36	7.45	7.66
	N3	7.5	7.5	7.45	7.07
	N3AB	7.58	7.67	7.7	7.58
Fall	N1	7.73	7.77	7.79	7.85
	N2	7.07	7.1	7.11	7.16
	N3	7.5	7.51	527	7.54
	N3AB	7.58	7.62	7.64	7.71
Winter	N1	7.73	7.75	7.77	7.73
	N2	7.07	7.08	7.09	7.06
	N3	7.5	7.53	7.54	7.48
	N3AB	7.58	7.64	7.76	7.58
Spring	N1	7.73	7.78	7.81	7.88
	N2	7.07	7.11	7.13	7.19
	N3	7.5	7.53	7.54	7.59
	N3AB	7.58	7.64	7.67	7.77

4. Discussion

The Eastern Oyster, *Crassostrea virginica*, is a critical foundational species dependent on freshwater inflow that creates habitat in the estuaries of Texas. Tres Palacios Bay and Carancahua Bay in the Lavaca-Colorado Estuary receive less freshwater inflow than northeastern estuaries of the Texas coast (Longley, 1994). A year-long detailed hydrological assay of multiple stations in Tres Palacios and Carancahua Bay from September 2015 to September 2016 found variable salinities due to an increased rainfall in the summer of 2016. Additionally, the bay bottom was mapped using side-scan sonar to validate existing oyster reefs during July 2016 (Dellapenna, 2016). During this mapping project, oysters were sampled for *Perkinsus marinus* (Dermo) infection. This activity produced an updated GIS map of the oyster reef locations in each bay (Fig. 22).

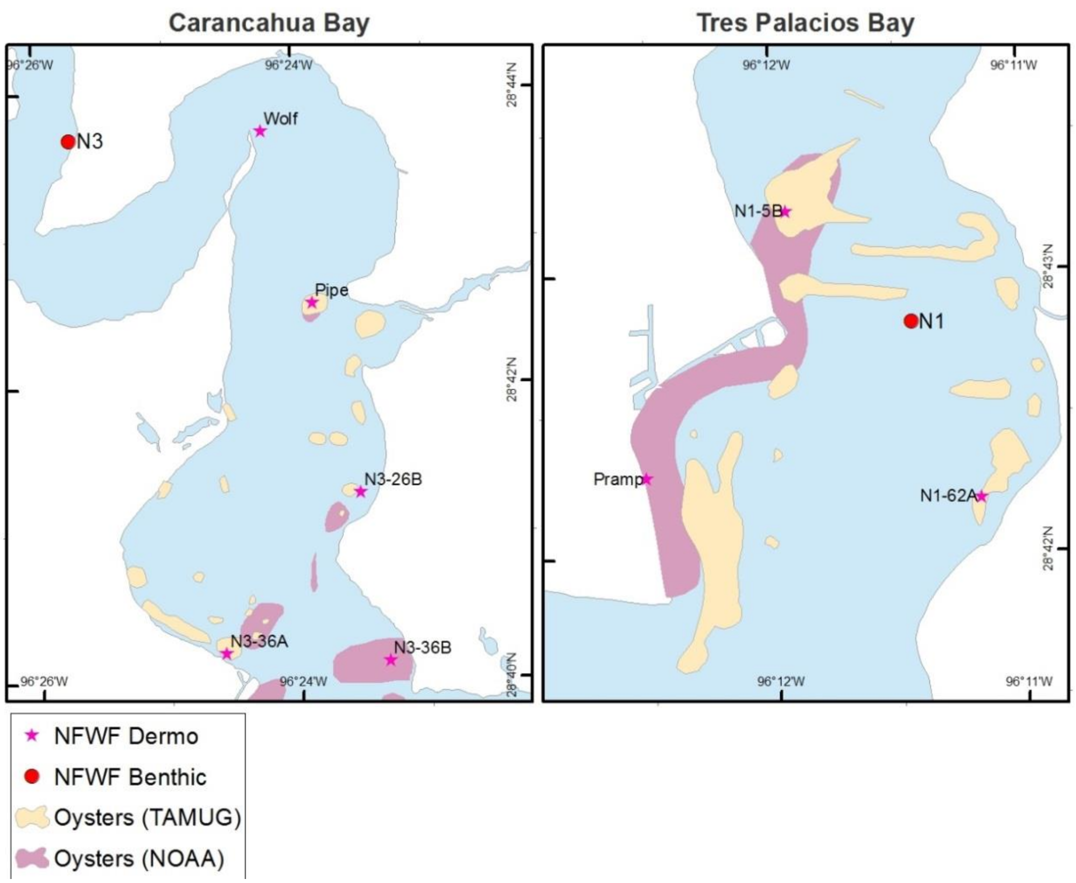

Fig. 22. Hydrographical and oyster reef sampling stations in Carancahua Bay and Tres Palacios Bay, Texas. Estimated oyster reef area as determined by NOAA is marked in purple. Identified reefs during July 2016 TAMUG mapping activities are identified in tan (Dellapenna, 2016).

This project aims to relate overall oyster health to inflow. In order to accomplish this task a habitat suitability index was created using factors previously known to affect overall oyster health. The habitat index was then matched to modeled historical inflow to multiple sample stations within Tres Palacios and Carancahua Bays. Results of this activity are there exist ideal inflow conditions to optimize specific oyster health indices within the reef locations.

For example, during the summer season station N1 in Tres Palacios requires 1,400 ac-ft/mo of freshwater to optimize the spawning activities of the Eastern Oyster (see Fig 21). Station N2, by contrast, would require 9,300 ac-ft/mo of freshwater inflow to optimize spawning.

These differences by upstream and downstream stations highlight the actual reef locations observed by the July 2016 mapping project (Fig. 22). For example, station N3 in Carancahua Bay according to the TXBLEND model output is historically too fresh on average to sustain oyster populations (A.2.). This is reflected in very low index scores for oyster mortality through sustained low salinities (SMI) and by low juvenile growth index values (JGI) during the summer months. Consequently, significant oyster populations were not observed near N3. By contrast in Tres Palacios Bay reefs were not located near the N2 station. This is similarly represented by TXBLEND model output and habitat index values being unfavorable due to higher on average salinities which affect the Dermo index (DRI) and overall growth (SGI).

The results of the run experiments yielded positive relationships for adding additional 500 to 1,000 ac-ft of inflow per summer month to each bay system. However, adding additional flows past 3,000 per year per summer decreased the overall index values due to salinities becoming lower than the ideal juvenile requirements (JGI). Adding additional flows to fall, spring, and winter had a very minimal effect at the quantities measured. This is due to the required flows to lower salinities to between 10 – 15 PSU is significant (> 40,000 ac-ft/mo) and beyond the capability of a purposeful management-based release.

The risks associated with oyster health and purposeful water release is also minimal. For example, it is extremely unlikely that a purposeful release could lower salinities to a contiguous monthly minimum below 2 PSU. Historically, only large flood events are able to achieve low salinity based die-off conditions to the oyster population. The only risk, however, is my lowering salinities below 20 PSU during summer which will affect the spawning months. This effect is evident during the historic 5,000 ac-ft/mo addition during the summer months.

A possible way to mitigate this risk is by adaptive release strategies. The flow scenarios in this study did not take into account the current inflow of the bay system before a release. A more realistic management release would be to supplement water during summer when the previous month was already dry and base salinities are approaching 35 PSU.

4.1. Limitations and Errors

The method employed of using habitat suitability indexes (HSI's) are especially problematic for oyster populations. As this activity was based on regressions the R^2 values are especially significant for validating the results. Oyster populations are difficult to regress, as evident of the R^2 values obtained in section 2. Additionally, validating HSI's are difficult as the purpose of an index is to translate multiple disparate quantitative frequencies into a qualitative average (Soniat and Brody, 1988). For example, the Copano Bay area used as a calibration system contains long-term data for oyster numbers, lengths, and Dermo intensity. During the years 2012 to 2014 oyster numbers and lengths remained high according to TPWD collections (TPWD, 2016). However, index values during this period are low because of higher on average salinities. This discrepancy between modeled output and observation can be explained by the *Perkinsus marinus* (Dermo) infection collections during this period. Oysters during this period were severely impacted by Dermo, which affected their overall health. The HSI, therefore, can be used as a qualitative tool to measure the overall health of oysters, but should not be interpreted as a hard qualitative value. The empirical methods employed in this study are instead used to detect a change in the system health.

Finally, the conclusions of this study rely heavily on modeled inflow and salinity using the TXBLEND hydrodynamic model (Matsumoto, 1993). The model was validated between 1987 to 2005 within an R^2 value of 0.61 and 0.70 of salinity observations at Caranacahau Bay and Tres Palacios Bay. Although these values are reasonable for a hydrodynamic model, a further regression of inflow to salinity compounds the uncertainties. A future direction of this work is further refinement of the regression techniques and additional calibration and validation of the TXBLEND model for the areas of study.

4.2. Conclusions

This study tested the effects of freshwater inflows supplements to Tres Palacios Bay and Carancahua Bay, Texas in altering overall oyster health. The results suggest that humanly achievable inflow additions can have a positive effect on *Crassostrea virginica* (Eastern Oyster) populations. By adding 500 ac-ft of freshwater monthly during June, July, and August overall oyster health is increased. The ideal time to increase existing freshwater inflow is during the summer months when *Crassostrea virginica* is spawning. As the spawning period is ideal during polyhaline salinities the burden of lowering salinities in the reef areas are manageable. Conversely, there is little risk of lowering oyster health by supplementing freshwater as the quantities required to lower salinity below optimal levels are physically unattainable to management.

References

Andrews, J. D. (1988). Epizootiology of the disease caused by the oyster pathogen Perkinsus marinus and its effects on the oyster industry. American Fisheries Society Special Publication, 18, 47-63.

Barnes, T. K., Volety, A. K., Chartier, K., Mazzotti, F. J., & Pearlstine, L. (2007). A habitat suitability index model for the eastern oyster (Crassostrea virginica), a tool for restoration of the Caloosahatchee Estuary, Florida. Journal of Shellfish Research, 26(4), 949-959.

Beck,M.W., R.D. Brumbaugh, L. Airoldi, A. Carranza, L.D. Coen, C. Crawford, O. Defeo, G.J. Edgar, B. Hancock, M. Kay, H. Lenihan, M.W. Luckenbach, C.L. Toropova, G. Zhang. 2009. Shellfish Reefs at Risk: A Global Analysis of Problems and Solutions. The Nature Conservancy, Arlington VA. 52 pp.

Bergquist, D.C., J.A. Hale, P. Baker and S.M. Baker. 2006. Development of ecosystem indicators for the Suwannee River estuary: oyster reef habitat quality along a salinity gradient. *Estuaries and Coasts* 29: 353–360.

Beseres Pollack J., A. Cleveland, T.A. Palmer, A.S. Reisinger, and P.A. Montagna. 2012. A restoration suitability index model for the eastern oyster (*Crassostrea virginica*) in the Mission-Aransas Estuary, TX, USA. *PLoS ONE* 7(7): e40839. doi:10.1371/journal.pone.0040839

Beseres Pollack, J., D. Yoskowitz, H.-C. Kim, P.A. Montagna. 2013. Role and value of nitrogen regulation provided by oysters (*Crassostrea virginica*) in the Mission-Aransas Estuary, Texas, USA. *PLoS ONE* 8(6): e65314. doi:10.1371/journal.pone.0065314

Buzan, D., W. Lee, J. Culbertson, N. Kuhn, and L. Robinson. 2006. Positive relationship between freshwater inflow and oyster abundance in Galveston Bay, Texas. *Estuaries and Coasts* 32: 206–212

Cake Jr, E. W. (1983). Habitat suitability index models: Gulf of Mexico American oyster (No. 82/10.57). US Fish and Wildlife Service.

Deepwater Horizon Natural Resource Damage Assessment Trustees. 2016. Deepwater Horizon oil spill: Final Programmatic Damage Assessment and Restoration Plan and Final Programmatic Environmental Impact Statement. Chapter 5. Restoring Natural Resources. Retrieved from http://www.gulfspillrestoration.noaa.gov/restoration-planning/gulf-plan

Dellapenna, T. 2016. Oyster Reef Mapping with Portions of Tres Palacios and Carancahua Bays in northern Matagorda Bay, Texas. Texas A&M University Galveston.

Longley, W.L., 1994. Freshwater Inflows to Texas Bays and Estuaries: Ecological Relationships and Methods for Determination of Needs. Texas Water Development Board and Texas Parks and Wildlife Department.

Matsumoto, J. 1993. User's Manual for the Texas Water Development Board's Hydrodynamic and Salinity Model, TxBLEND. Texas Water Development Board, Austin, Texas.

Montagna, P.A., T.A. Palmer, and J. Beseres Pollack. 2013. Hydrological Changes and Estuarine Dynamics. SpringerBriefs in Environmental Sciences, New York, New York. 94 pp.

Pollack, J.B., H.-C. Kim, E.K. Morgan, and P.A. Montagna. 2011. Role of flood disturbance in natural oyster (*Crassostrea virginica*) population maintenance in an estuary in South Texas, USA. *Estuaries and Coasts* 34:187–197.

Ray S.M. 1966. A review of the culture method for detecting *Dermocystidium marinum*, with suggested modifications and precautions. *Proceedings of the National Shellfisheries Association* 54: 55–69.

Ray S. M. 2016 Oyster Sentinel Database. Retrieved from www.oystersentinel.org. ACCESSED OCT, 2016.

Soniat, T. M., & Brody, M. S. (1988). Field validation of a habitat suitability index model for the American oyster. Estuaries, 11(2), 87-95.

Texas Parks and Wildlife Department. 2016. Marine resource monitoring program: Coastal fisheries database. Austin, Texas

Turner, E.L. and P.A. Montagna. 2017. The Max Bin regression method to identify maximum bioindicator responses to ecological drivers. *Ecological Informatics* In Press

Turner, R.E. 2006. Will lowering estuarine salinity increase Gulf of Mexico oyster landings? *Estuaries and Coasts* 29: 345–352.

zu Ermgassen, P.S.E., M.D. Spalding, B. Blake, L.D. Coen, B. Dumbauld, S. Geiger, J.H. Grabowski, R. Grizzle, M. Luckenbach, K.A. McGraw, B. Rodney, J.L. Ruesink, S.P. Powers, and R.D. Brumbaugh. 2012. Historical ecology with real numbers: past and present extent and biomass of an imperiled estuarine ecosystem. *Proceedings of the Royal Society B* 279: 3393–3400.

zu Ermgassen, P.S.E., M.D. Spalding, R.E. Grizzle, and R.D. Brumbaugh. 2013. Quantifying the loss of a marine ecosystem service: filtration by the eastern oyster in US estuaries. *Estuaries and Coasts* 36: 36-43.

5. Appendices

5.1. A.1. SAS code for the Oyster Habitat Suitability Index

```
/* Texas Gulf Coast Oyster Habitat Suitability Index
Evan Lee Turner
evan.turner@tamucc.edu
Oct 2016
*/
proc datasets lib=work kill nolist memtype=data;
quit;
%let Dermoriskfile = cop.Dermoindex;
%let estuaryfile = cop.monthly;
%let SM =  exp(-0.5*(log(sal/10)/1.5)**2);
%let SG = exp(-0.5*(log(sal/12)/0.5)**2);
%let DR = exp(-0.5*((TDRM/2)**2.5));
%let JG = exp(-0.5*(log(sal/21.65)/0.30511)**2);
/* prepare the Dermo risk model output */
proc sort data=&Dermoriskfile  out=Dermorisk; by date; run;
proc means data=Dermorisk noprint;
class date;
format date year.;
var TDRM;
output out=Dermorisk2(  drop=_FREQ_ _TYPE_ ) mean=TDRM;
run;
data Dermoindex;
set Dermorisk2;
if date EQ '.' then delete;
DRI = &DR;
year = put(date,year.);
keep DRI year;
run;
data HSImonthly;
set &estuaryfile;
month = put(date,month2.);
year = put(date,year.);
JGI = &JG;
SMI = &SM;
if month LT 6 or month GT 9 then JGI = '.';
run;
proc means data=HSImonthly noprint;
var sal JGI SMI;
by year;
output out=HSIyear(drop =  _type_ _freq_ sal_min smi_mean jgi_min) mean= min= /autoname;
run;
```

```
data HSIyear;
merge HSIyear Dermoindex;
by year;
sal = sal_mean;
SGI = &SG;
JGI = JGI_mean;
SMI = SMI_min;
HSI = (SGI + JGI + SMI + DRI) * 2.5;
HSI = (SGI * JGI * SMI * DRI) ;
HSI = (SGI + JGI + SMI + DRI) * 2.5;
drop sal_mean JGI_mean SMI_min;
run;
```

5.2. A.2. Habitat Suitability Index and sub-index values for Carancahua and Tres Palacios Bay stations N1, N2, N3, and N3AB from Nov, 1986 to Dec, 2015.

Year	Station	Avg. Salinity (PSU)	Avg. Inflow (Ac-ft/Mo)	HSI Sub-Indices				Yearly HSI
				JGI	SMI	DRI	SGI	
1986	N1	10.8	32096	.	0.99	1.00	0.98	.
1986	N2	20.3	32096	.	0.89	1.00	0.58	.
1986	N3	4.9	43984	.	0.87	1.00	0.20	.
1986	N3AB	10.6	43984	.	1.00	1.00	0.97	.
1987	N1	18.4	11695	0.53	0.82	0.98	0.69	7.56
1987	N2	24.9	11695	0.83	0.76	0.94	0.35	7.17
1987	N3	12.7	15291	0.29	0.71	1.00	0.99	7.47
1987	N3AB	18.3	15291	0.47	0.83	0.98	0.70	7.46
1988	N1	24.1	1889	0.89	0.82	0.93	0.38	7.55
1988	N2	28.5	1889	0.60	0.77	0.90	0.22	6.23
1988	N3	20.2	2025	0.99	0.87	0.97	0.58	8.51
1988	N3AB	25.1	2025	0.82	0.80	0.92	0.34	7.22
1989	N1	23.6	5643	0.83	0.78	0.93	0.40	7.35
1989	N2	29.4	5643	0.44	0.71	0.88	0.20	5.58
1989	N3	19.9	4193	0.83	0.83	0.97	0.60	8.07
1989	N3AB	25.3	4193	0.74	0.76	0.92	0.33	6.89
1990	N1	21.1	6875	0.96	0.81	0.97	0.53	8.19
1990	N2	26.8	6875	0.71	0.76	0.92	0.28	6.65
1990	N3	16.7	9264	0.54	0.87	0.99	0.80	8.02
1990	N3AB	22.1	9264	0.91	0.80	0.97	0.48	7.90
1991	N1	16.0	21756	0.95	0.85	0.98	0.85	9.07
1991	N2	22.6	21756	0.82	0.79	0.95	0.45	7.50
1991	N3	10.5	24111	0.32	0.83	1.00	0.97	7.78
1991	N3AB	16.1	24111	0.89	0.86	0.99	0.84	8.95
1992	N1	12.1	33747	0.55	0.59	0.99	1.00	7.83
1992	N2	19.4	33747	0.64	0.77	0.97	0.63	7.52
1992	N3	6.8	43582	0.33	0.11	1.00	0.53	4.94
1992	N3AB	11.5	43582	0.51	0.58	0.99	1.00	7.71
1993	N1	14.2	21111	0.51	0.82	0.99	0.95	8.18
1993	N2	21.1	21111	0.61	0.78	0.97	0.53	7.22
1993	N3	10.5	26847	0.42	0.62	1.00	0.97	7.52
1993	N3AB	15.1	26847	0.47	0.81	0.99	0.90	7.92
1994	N1	15.7	19642	0.57	0.89	0.99	0.87	8.29
1994	N2	22.2	19642	0.93	0.83	0.95	0.47	7.96
1994	N3	13.4	12732	0.39	0.93	1.00	0.98	8.24
1994	N3AB	18.0	12732	0.87	0.87	0.98	0.72	8.60
1995	N1	16.2	20059	0.67	0.85	0.98	0.83	8.34
1995	N2	23.5	20059	0.82	0.78	0.94	0.40	7.37

Year	Station	Avg. Salinity (PSU)	Avg. Inflow (Ac-ft/Mo)	HSI Sub-Indices				Yearly HSI
				JGI	SMI	DRI	SGI	
1995	N3	11.1	21443	0.41	0.79	1.00	0.99	7.96
1995	N3AB	16.7	21443	0.64	0.85	0.98	0.81	8.19
1996	N1	20.6	10995	0.75	0.81	0.97	0.56	7.70
1996	N2	26.8	10995	0.78	0.76	0.91	0.27	6.83
1996	N3	15.5	11045	0.37	0.85	0.99	0.88	7.74
1996	N3AB	21.0	11045	0.70	0.79	0.96	0.53	7.47
1997	N1	12.0	38294	0.71	0.79	1.00	1.00	8.74
1997	N2	18.7	38294	0.84	0.81	0.98	0.68	8.29
1997	N3	8.1	47417	0.35	0.34	1.00	0.73	6.04
1997	N3AB	12.2	47417	0.66	0.74	1.00	1.00	8.49
1998	N1	16.7	21389	0.61	0.79	0.97	0.80	7.92
1998	N2	23.0	21389	0.57	0.73	0.93	0.43	6.67
1998	N3	11.9	27698	0.72	0.42	0.99	1.00	7.82
1998	N3AB	16.8	27698	0.58	0.78	0.97	0.80	7.82
1999	N1	21.7	5768	0.76	0.81	0.97	0.50	7.60
1999	N2	27.3	5768	0.76	0.76	0.91	0.26	6.72
1999	N3	16.5	6900	0.54	0.88	0.99	0.82	8.05
1999	N3AB	22.2	6900	0.88	0.81	0.96	0.47	7.79
2000	N1	22.3	8823	0.83	0.79	0.96	0.46	7.60
2000	N2	28.8	8823	0.66	0.74	0.90	0.21	6.29
2000	N3	18.5	7198	0.70	0.84	0.98	0.69	8.04
2000	N3AB	24.2	7198	0.76	0.78	0.95	0.37	7.14
2001	N1	17.2	19436	0.69	0.81	0.97	0.77	8.12
2001	N2	23.9	19436	0.55	0.74	0.93	0.38	6.51
2001	N3	12.3	24447	0.63	0.56	0.99	1.00	7.96
2001	N3AB	17.5	24447	0.62	0.78	0.97	0.75	7.80
2002	N1	15.9	20895	0.54	0.84	0.99	0.85	8.06
2002	N2	22.2	20895	0.92	0.80	0.94	0.47	7.82
2002	N3	12.0	24339	0.35	0.46	1.00	1.00	7.00
2002	N3AB	16.9	24339	0.72	0.79	0.98	0.79	8.19
2003	N1	18.1	10367	0.74	0.83	0.97	0.71	8.13
2003	N2	24.4	10367	0.79	0.77	0.93	0.37	7.14
2003	N3	12.8	13476	0.35	0.90	1.00	0.99	8.10
2003	N3AB	18.4	13476	0.87	0.84	0.97	0.69	8.43
2004	N1	12.7	37939	0.49	0.86	1.00	0.99	8.36
2004	N2	20.0	37939	0.65	0.82	0.98	0.60	7.59
2004	N3	9.4	40145	0.24	0.57	1.00	0.88	6.74
2004	N3AB	14.0	40145	0.47	0.88	1.00	0.95	8.24
2005	N1	19.0	8076	0.92	0.83	0.97	0.66	8.46
2005	N2	24.7	8076	0.73	0.77	0.93	0.35	6.95
2005	N3	13.5	12682	0.52	0.67	1.00	0.97	7.89

Year	Station	Avg. Salinity (PSU)	Avg. Inflow (Ac-ft/Mo)	HSI Sub-Indices				Yearly HSI
				JGI	SMI	DRI	SGI	
2005	N3AB	19.0	12682	0.91	0.83	0.97	0.66	8.41
2006	N1	19.7	13682	0.56	0.82	0.98	0.61	7.43
2006	N2	26.2	13682	0.91	0.76	0.93	0.29	7.23
2006	N3	14.4	22299	0.06	0.81	1.00	0.94	7.00
2006	N3AB	19.9	22299	0.51	0.80	0.98	0.60	7.23
2007	N1	12.5	30213	0.10	0.43	1.00	1.00	6.31
2007	N2	19.4	30213	0.58	0.83	0.98	0.63	7.56
2007	N3	8.1	39217	0.00	0.06	1.00	0.74	4.50
2007	N3AB	12.7	39217	0.07	0.50	1.00	0.99	6.40
2008	N1	22.4	6691	0.84	0.80	0.94	0.46	7.59
2008	N2	28.5	6691	0.49	0.73	0.89	0.22	5.85
2008	N3	18.3	6338	0.97	0.86	0.97	0.70	8.74
2008	N3AB	24.0	6338	0.74	0.78	0.93	0.38	7.07
2009	N1	24.5	4958	0.63	0.74	0.92	0.36	6.61
2009	N2	29.7	4958	0.39	0.69	0.88	0.19	5.40
2009	N3	21.6	2584	0.87	0.79	0.94	0.50	7.76
2009	N3AB	26.5	2584	0.56	0.72	0.90	0.29	6.18
2010	N1	15.4	17243	0.45	0.87	0.99	0.88	8.00
2010	N2	21.7	17243	0.90	0.81	0.96	0.50	7.92
2010	N3	9.7	28000	0.03	0.58	1.00	0.91	6.30
2010	N3AB	14.5	28000	0.30	0.87	1.00	0.93	7.72
2011	N1	25.4	1710	0.72	0.76	0.92	0.33	6.82
2011	N2	30.0	1710	0.44	0.71	0.88	0.19	5.54
2011	N3	20.9	2448	0.94	0.82	0.95	0.54	8.14
2011	N3AB	26.2	2448	0.66	0.75	0.91	0.30	6.55
2012	N1	19.9	11209	0.82	0.83	0.98	0.60	8.09
2012	N2	26.6	11209	0.79	0.77	0.93	0.28	6.94
2012	N3	15.4	10594	0.43	0.90	1.00	0.88	8.03
2012	N3AB	21.0	10594	0.79	0.83	0.98	0.53	7.83
2013	N1	22.8	4674	0.86	0.80	0.94	0.44	7.60
2013	N2	28.3	4674	0.55	0.74	0.90	0.23	6.03
2013	N3	18.3	4467	0.95	0.87	0.97	0.70	8.72
2013	N3AB	23.7	4467	0.83	0.79	0.93	0.39	7.38
2014	N1	23.3	3308	0.93	0.82	0.94	0.41	7.78
2014	N2	28.3	3308	0.64	0.75	0.90	0.23	6.31
2014	N3	18.9	2915	0.89	0.88	0.98	0.66	8.54
2014	N3AB	24.1	2915	0.90	0.81	0.94	0.38	7.57
2015	N1	15.9	20366	0.62	0.87	0.99	0.85	8.34
2015	N2	23.3	20366	0.82	0.81	0.96	0.41	7.50
2015	N3	10.4	28012	0.10	0.62	1.00	0.96	6.70
2015	N3AB	16.0	28012	0.47	0.87	0.99	0.85	7.97